Supplementary Information (SI) for Environmental Science: Nano.

Supporting Information

Eco-friendly nanobioengineered CuO platform mediated through *Ficus religiosa* latex for malathion detection

Kshitij RB Singh[1*], Pooja Singh[2], Shyam S. Pandey[1*]

[1]Graduate School of Life Science and Systems Engineering, Kyushu Institute of Technology, 2-4 Hibikino, Wakamatsu, Kitakyushu (808-0196), Japan.

[2]Department of Biotechnology, Indira Gandhi National Tribal University, Amarkantak, Madhya Pradesh (484886), India.

[*]Corresponding author (**S.S.P.**: shyam@life.kyutech.ac.jp; **K.R.B.S.**: krbs09@gmail.com)

S1. Materials

Copper (II) sulphate pentahydrate ($CuSO_4.5H_2O$; MW: 249.68 g mol^{-1}), potassium hexacyanoferrate (II) trihydrate ($C_6FeK_4N_6 \cdot 3H_2O$; MW: 422.39 g mol^{-1}; Product cat no.: 1.93686.0521), potassium hexacyanoferrate (III) ($C_6FeK_3N_6$; MW: 329.25 g mol^{-1}; Product cat no.: 1.93667.0521), Malathion ($C_{10}H_{19}O_6PS_2$; MW: 330.36; Product cat no.: 36143-100MG), sodium chloride (NaCl; MW: 58.44 g mol^{-1}; Product cat no.: S9888), Choline oxidase from *Alcaligenes* sp. (≥10 units/mg solid; CAS No. : 9028-67-5; EC No.: 232-840-0; Product cat no.: C5896-50UN) and Whatman filter paper Grade-1, all were purchased from Sigma-Aldrich, USA. Sodium hydroxide (NaOH; MW: 40.00 g mol^{-1}; CAS no.: 1310-73-2) and ammonia liquor (NH_3; MW: 17.03 g mol^{-1}; CAS no.: Q16225) were obtained from Qualigens, Thermo Fisher Scientific, USA. Disodium phosphate ($Na_2HPO_4 \cdot H_2O$; MW: 177.99; CAS No.: 10028-24-7) and monosodium phosphate (NaH_2PO_4; MW: 119.98; CAS No.: 7558-80-7) were procured from Himedia, India. The ITO sheets (surface resistivity 30–60 Ω sq^{-1}) were procured from Sigma-Aldrich, USA, for the electrophoretic deposition of prepared nanoparticles. Milli-Q water (18 Ω resistivity; Millipore, USA) was used in all the experimental works. In addition, the utilized phosphate buffer saline (PBS) in this work contains 0.9% saline NaCl and 5 mM of ferric ferrocyanide $(Fe(CN)_6)^{3-/4}$. *Ficus religiosa* stem latex was collected from Indira Gandhi National Tribal University, Amarkantak, Madhya Pradesh, India.

S2. Instrumentation

Infrared spectra were recorded with a Nicolet iS5, Thermo Fisher Scientific, USA, in the spectral range 500-4000cm^{-1} of the synthesized nanoparticles. UV-visible spectroscopy was performed by using a UV-1800 Shimadzu, Japan, in the wavelength range of 200-400 nm to investigate the NP's optical properties. XRD techniques examined the structure and crystalline size of CuO NPs by using an X-ray diffractometer (D8 Advance, Bruker, USA) with a Cu-Kα (λ = 1.5406 Å) in the 2θ angles ranging from 30 to 80°. Further, SEM and energy dispersive

X-ray analysis (EDX) were performed to determine surface morphology and element confirmation of synthesized NPs by using Thermo Scientific, USA Quattro S., having an EDX attachment of EDS Ultradry. X-ray photoelectron spectroscopy (XPS; PHI 5000 Versa Probe III, using the Al Kα radiation, hν= 1486·6 eV, and scanning of Al Kα X-ray spot size is adjustable from 10 to 200 μm, and scanning dimensions up to 1.4 mm. Further, the electrochemical Malathion sensing studies of the fabricated ChO-CuO NPs/ITO nanobioengineered electrode were performed by the EmStat4S electrochemical workstation of PalmSens, Netherlands, using three three-electrode system. This workstation is gifted by *Class One Systems S&T Pvt. Ltd.* for performing electrochemical studies in Pandey Laboratory at Kyushu Institute of Technology, Japan.

For the 2D positional mapping of the fabricated electrode to assess the uniformity of CuO NPs deposition, a single-beam, multi-channel detector system equipped with a precision X-Y stage controller was employed (**Figure S1A**). This setup enables the electronic absorption spectrum of the sample to be recorded at specific locations. The core component of this system is a photonic multi-channel analyzer (PMA, C7473-36, Hamamatsu Photonics, Japan), which incorporates a Czerny-Turner spectrograph and thermoelectrically cooled back-thinned charge-coupled device (BT-CCD) photodetectors with an electronic shutter function. To facilitate multichannel spectroscopy, the PMA employs an array of 1024 photosensitive BT-CCD units. The diffraction grating and multi-channel detector are securely fixed to ensure consistent photodetection performance. An external digital function generator (DF1906, NF Corporation, Japan) controlled the electronic shutter attached to the photodetector unit. Illumination was provided by a halogen lamp (Megalight 100, Schott, IBE SMT Equipment, Magnolia) paired with an optical fiber and focusing lens, covering a wavelength range of 350–900 nm. The sample stage (Stepping motor-drive SGSP stage/TSDM series, Sigma Koki, Japan) was positioned in the X-Y plane, perpendicular to the alignment axis of the light source and

detector. The stage was set 10 cm from the focus lens to achieve optimal illumination intensity and ease of handling. Motion in the X-Y plane was managed via a 2D stage controller (Mark-12, Sigma Koki, Japan), which interfaced with the stage using a 2-axis micro-driver. To analyze the behavior quantitatively, the beam from the halogen lamp, with a width of 5 mm, was directed vertically onto the sample. The transmitted light was captured by an optical fiber linked to the PMA, where it was collimated and dispersed into constituent wavelengths by the spectrograph. The multichannel photodetector received the dispersed signal. The PMA was connected to a computer to integrate the detector output and analyze the absorption spectra. To improve the signal-to-noise ratio, five consecutive measurements were averaged. The recorded spectra were then integrated for each measured point. To achieve precise film homogeneity mapping, the spacing between measurement points and their coverage area needed to be minimized. The PMA fiber's effective light-receiving area, with a diameter of 1 mm, determined the smallest scan area. For this mapping, a mask with a 0.5 mm diameter, a stage speed of 1 mm/s, and a shutter frequency of 5 Hz with a 10% duty cycle was utilized. These settings enabled measurements over the electrode area of 2 mm (equivalent to the fabricated electrode's 0.25 cm^2 area, **Figure S1B**) to evaluate the uniformity of deposition achieved through electrophoretic deposition.

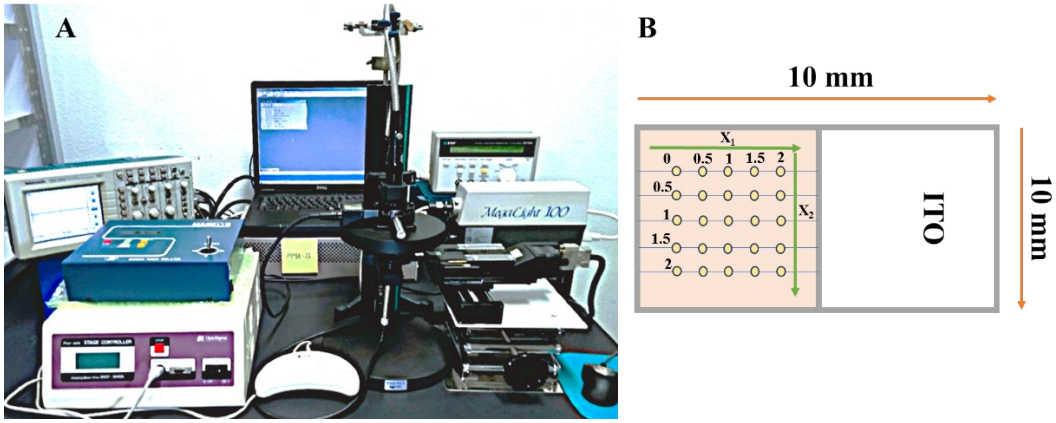

Figure S1. ***A)*** *Picture of our in-lab developed setup for 2D positional mapping, and* ***B)*** *the area scanned on our fabricated electrode from 0 to 2mm covering X_1 and X_2 points.*

S3. Synthesis of CuO NPs

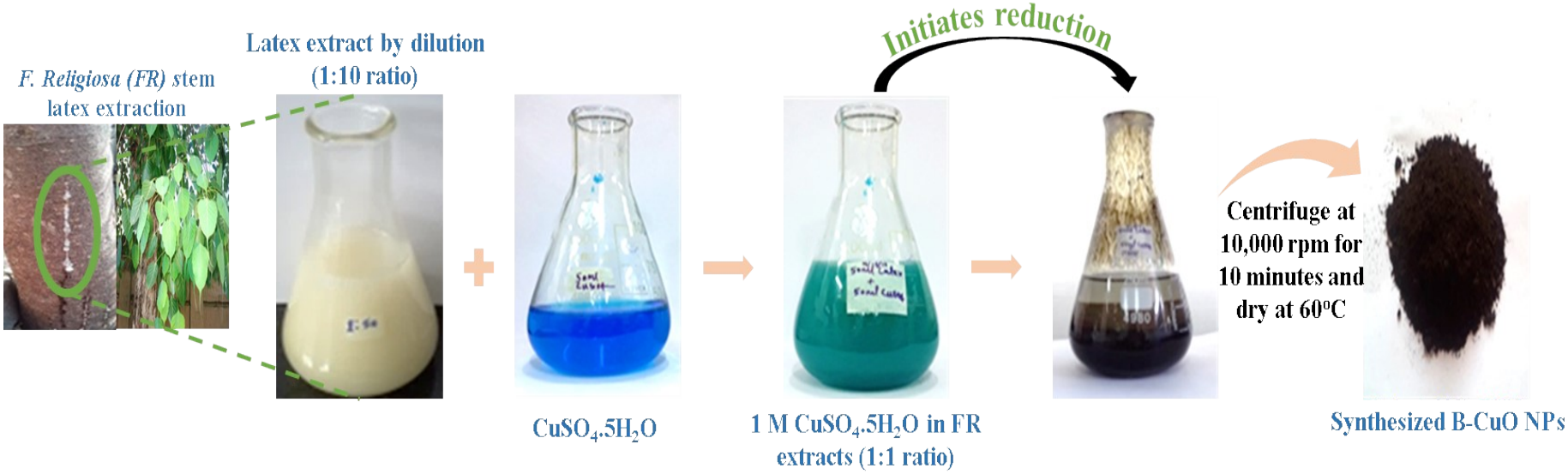

Figure S2. *Process of CuO NPs synthesis.*

S4. XRD crystallite size calculation of CuO NPs

Table S1. *Crystallite size calculation.*

Parameters		**Calculations**		**D (nm)**	**Average D (nm)**
K	**λ**	**Peak position 2θ (°)**	**FWHM β (°)**		
0.94	1.5406	32.34	0.549	15.736	21.22
		34.21	0.303	28.651	
		35.66	0.359	24.278	
		38.93	0.424	20.755	
		48.94	0.340	26.812	
		53.62	0.360	25.824	
		58.36	0.457	20.795	
		61.76	0.448	21.580	
		66.44	1.177	8.426	
		68.24	0.525	19.090	
		72.47	0.354	29.058	
		75.42	0.768	13.656	

S5. TEM-EDS

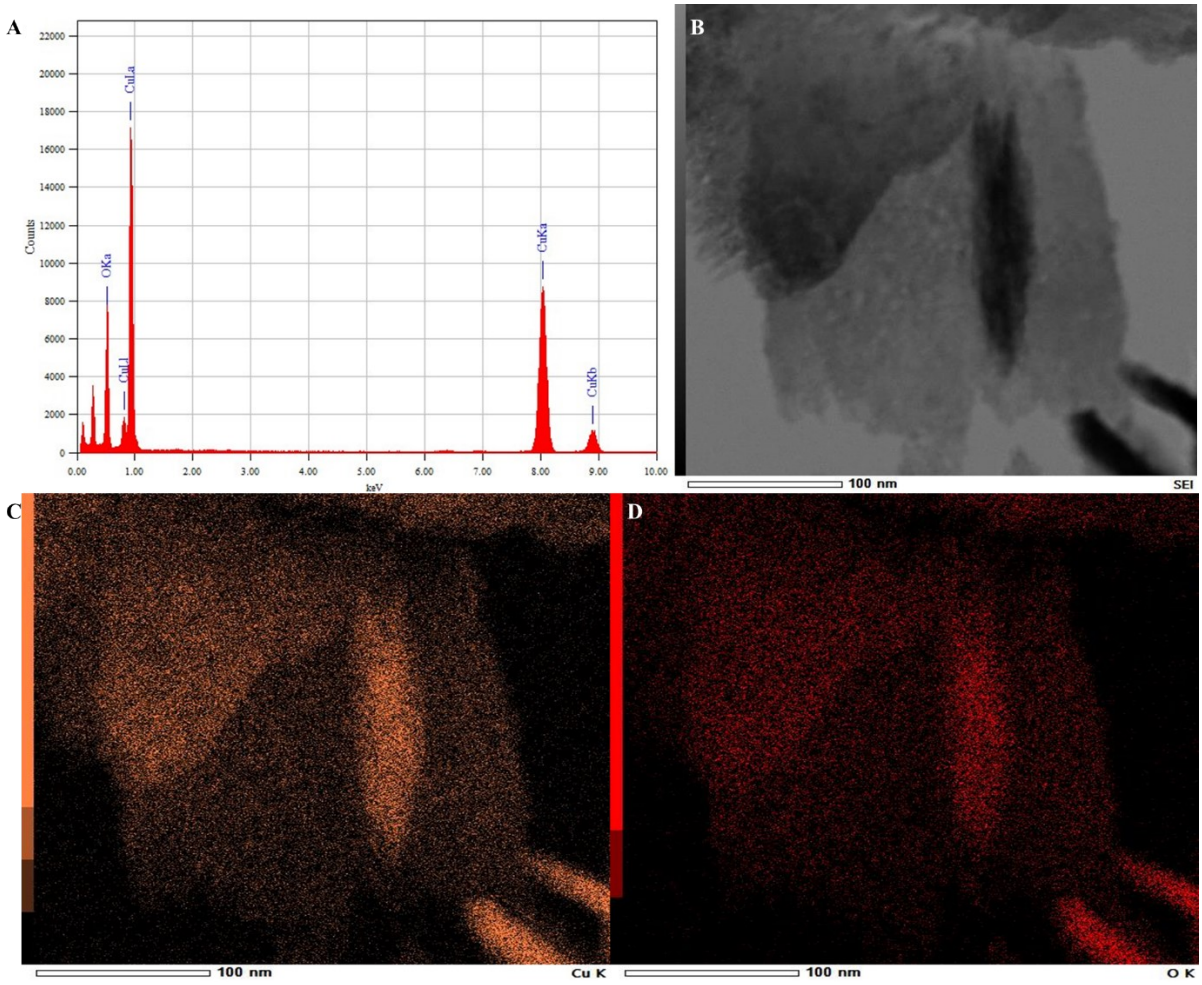

Figure S3. *TEM-based EDS spectrum **(A)** confirms Cu and O presence, and elemental mapping **(B-D)** displays homogeneous Cu and O distribution.*

S6. Details of Variables in Equations (Kinetics Studies)

This section provides the details of variables used in **Eq. 6 to 8**, for calculating K_s in **Eq. 6** the variables '*m*' represents the peak-to-peak separation (0.29 V), '*v*' is the scan rate (50 mV s^{-1}), '*n*' denotes the number of electrons transferred in the redox process (n = 1), '*T*' is the temperature (27 °C), '*R*' is the gas constant (8.314 J mol^{-1} K^{-1}), and '*F*' is the Faraday constant (96,485 C mol^{-1}). For **Eq. 7**, applied to calculate the *D* in a one-electron transfer and quasi-reversible electrochemical reaction system, 'α' is the charge transfer coefficient (0.967), calculated using **Eq. S1** with I_{pa} (1.043 mA) and I_{pc} (-1.009 mA) values at a 50 mV s^{-1} scan rate. '*C*' represents the mediator concentration (0.000005 mol cm^{-3}), while other variables (R, F, T, n, ν) remain consistent with **Eq. 6**. Finally, in **Eq. 8**, used for determining Υ, '*A*' denotes the electrode surface area (0.25 cm^2), with other variables identical to those in **Eqs. 6 & 7**. These equations collectively highlight the electrochemical kinetics of the fabricated ChO-CuO NPs/ITO nanobioengineered electrode, underscoring its potential for effective malathion sensing.

$$\alpha = \frac{I_{pc}}{I_{pa}} \qquad \textbf{Eq. S1}$$

S7. Reproducibility, Stability, and Real Sample Analysis

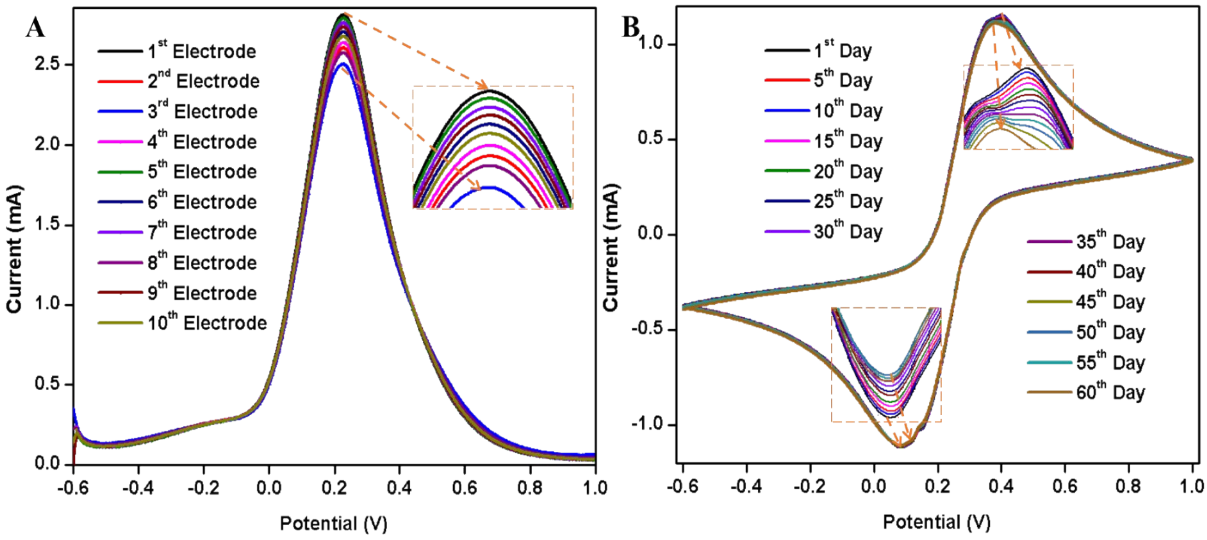

Figure S4. ***A)*** *DPV Scan of reproducibility analysis and* ***B)*** *CV scan of stability analysis.*

Table S2. *Detection of malathion in spiked soil samples (Real sample analysis).*

Concentration of malathion added (µM)	**Concentration of malathion determined in soil samples (µM)**	**Recovery (%)**	**RSD (%)**
10	9.87	98.76	0.43
60	58.86	98.11	0.99
100	98.74	98.74	0.49
140	136.89	97.78	0.75

S8. Absorbance data of 2D positional mapping

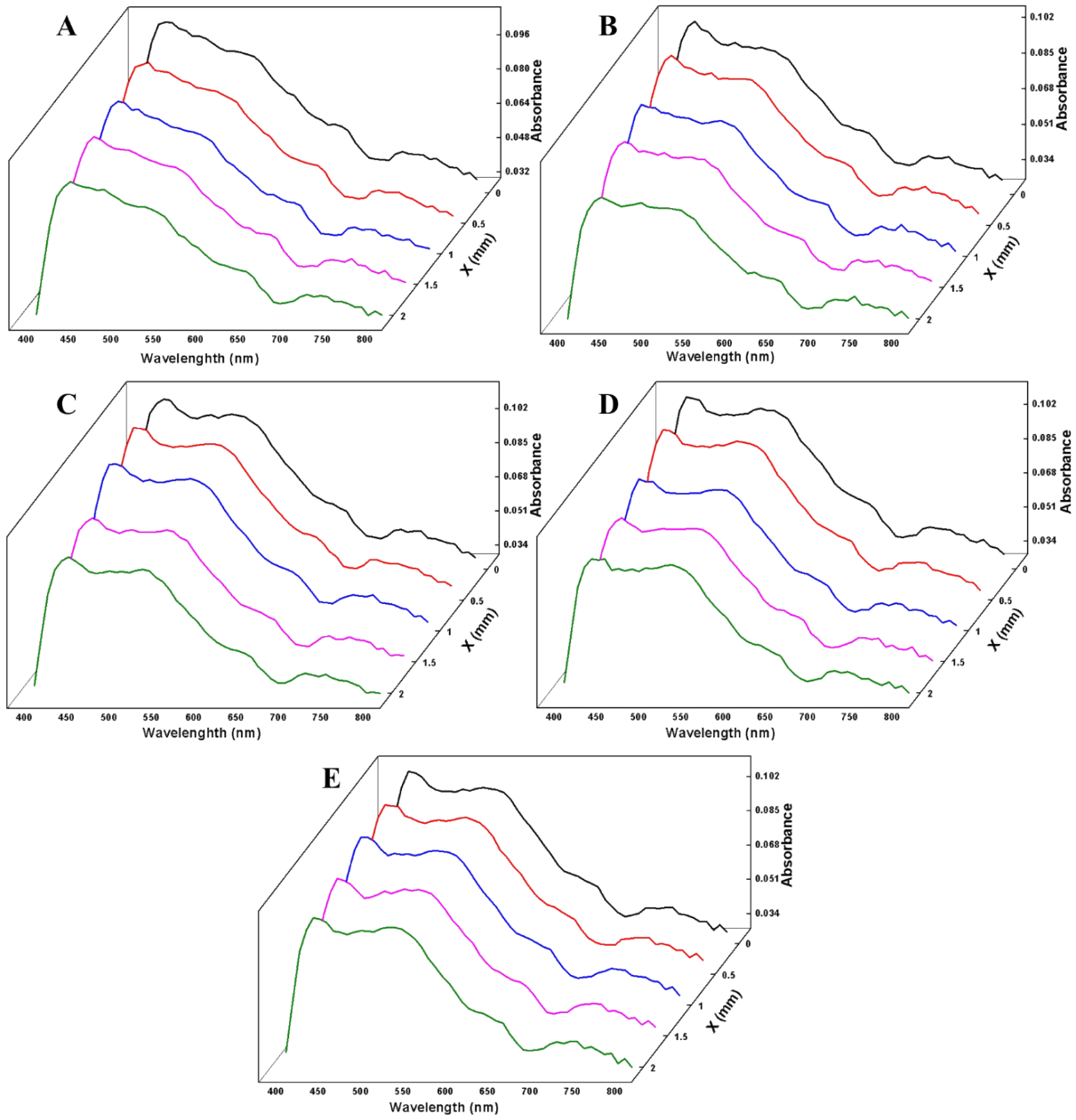

Figure S5. *Electronic absorbance spectra obtained for fabricated CuO NPs/ITO electrode at fixed starting (X_2) points:* ***A)*** *0 mm,* ***B)*** *0.5 mm,* ***C)*** *1 mm,* ***D)*** *1.5 mm, and* ***E)*** *2 mm towards X_1 direction as depicted in* ***Figure S1B****.*

Table S3. *Extracted absorbance values from the 2D positional mapping graph* ***Figure 7F,*** *along with absorbance change percentage, minimum & maximum absorbance, and RSD percentage.*

X_1 / X_2	**0 mm**	**0.5 mm**	**1 mm**	**1.5 mm**	**2 mm**
	Absorbance				
0 mm	0.11001	0.10836	0.11469	0.11427	0.11262
0.5 mm	0.10698	0.1062	0.11565	0.11365	0.11177
1 mm	0.10154	0.09864	0.11435	0.10405	0.11026
1.5 mm	0.09845	0.0951	0.10159	0.09967	0.10537
2 mm	0.09232	0.08379	0.09769	0.09611	0.10185
Absorbance Maximum	0.11001	0.10836	0.11565	0.11427	0.11262
Absorbance Minimum	0.09232	0.08379	0.09769	0.09611	0.10185
Absorbance Change %	16.07792	22.67642	15.52786	15.89395	9.56281
RSD (%)	6.86227	9.96162	7.79964	7.74911	4.24469

S9. Fabricated electrodes characterization

The electronic absorption spectra shown in **Figure S5** provide insights into the successful immobilization of Choline Oxidase (ChO) enzyme on CuO NPs/ITO electrodes. The black line represents the spectrum of the CuO NPs/ITO electrode, whereas the red line corresponds to the ChO-CuO NPs/ITO nanobioengineered electrode. The addition of ChO results in distinctive absorption features associated with enzyme immobilization. The absorption spectrum of the CuO NPs thin film is consistent with its established optical properties, as reported in the literature (Hussein M. Hussein, 2023). Spin-coated CuO thin films exhibit high absorption in the visible range, with features that can be attributed to the bandgap and optical transitions such as d-d transitions in CuO nanocrystals. These properties, along with the enhanced crystallinity and morphology, play a crucial role in its optoelectronic behavior. The observed π-π^* transition, marked in the spectra of the ChO-CuO NPs/ITO nanobioengineered electrode at 290 nm, is indicative of aromatic or conjugated systems within the ChO enzyme. This transition is characteristic of interactions involving aromatic amino acid residues or similar structures present in enzymes(Fan and Gadda, 2005; Gadda, 2020). Furthermore, the n-π^* transition, another key feature, is attributed to functional groups such as C-N and P=O, which involve the excitation of non-bonding electrons to anti-bonding π^* orbitals. These transitions provide evidence of the specific chemical interactions occurring due to enzyme immobilization on the CuO nanostructures (Gadda, 2020). The combination of spectral features confirms the effective immobilization of ChO on the CuO NPs/ITO surface. The presence of π-π^* and n-π^* transitions signifies robust binding facilitated by the functional groups within ChO, which interact with the CuO NPs. These findings demonstrate that the nanoengineered electrode successfully integrates enzyme functionality with CuO nanostructures, enhancing its potential for biosensing applications.

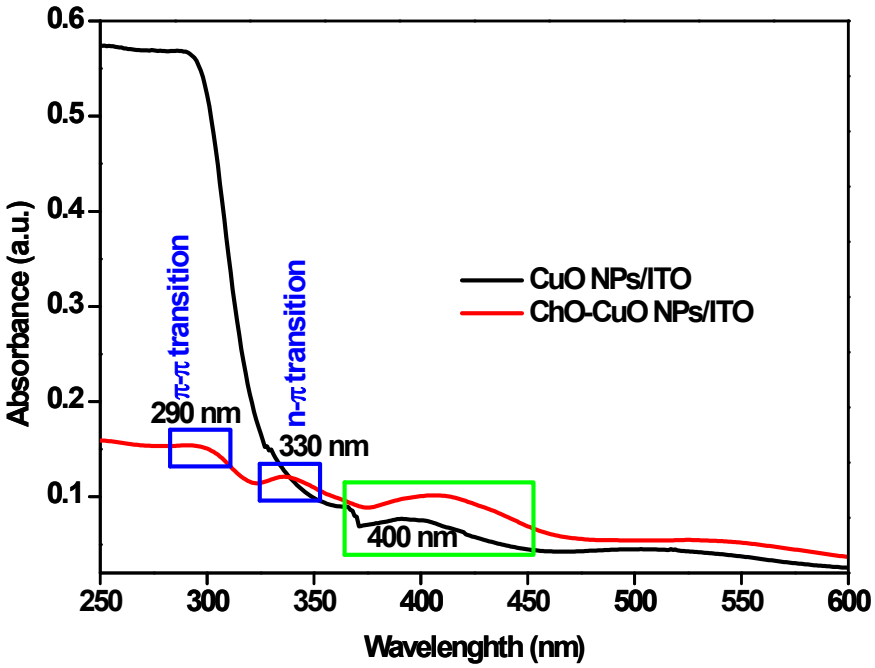

Figure S6. *Electronic absorption spectra of CuO NPs/ITO electrode (black line) and ChO-CuO NPs/ITO nanobioengineered electrode.*

References

Fan, Gadda, G., 2005. On the Catalytic Mechanism of Choline Oxidase. J Am Chem Soc 127, 2067–2074. https://doi.org/10.1021/ja044541q

Gadda, G., 2020. Choline oxidases. pp. 137–166. https://doi.org/10.1016/bs.enz.2020.05.004

Hussein M. Hussein, 2023. Fabricating and Synthesizing Spin Coated CuO Thin Film as Absorber Layer in Optoelectronic Applications. Protection of Metals and Physical Chemistry of Surfaces 59, 422–427. https://doi.org/10.1134/S2070205123700491